Int. J. Electrochem. Sci., 10 **(2015)** 5048 - 5060

International Journal of
ELECTROCHEMICAL
SCIENCE
www.electrochemsci.org

An Improvement of Electrochemical Performance of $Li_{1.2}Mn_{0.54}Ni_{0.13}Co_{0.13}O_2$ by blending with $Na_{0.6}[Li_{0.2}Mn_{0.8}]O_2$

He Huang[1], *Guo-Biao Liu*[2], *Jin-Hua Wu*[1,3], *Heng Liu*[1,*]

[1] College of Materials Science and Engineering, Sichuan University, Chengdu 610064, China
[2] Chengdu Green Energy and Green Manufacturing Technology R&D Center, Chengdu Development Center of Science and Technology, China Academy of Engineering Physics, Chengdu, 610207, China
[3] Department of Materials Engineering, Sichuan College of Architectural Technology, Deyang 618000, China
[*]E-mail: h_liu@scu.edu.cn

Received: 9 March 2015 / *Accepted:* 11 April 2015 / *Published:* 28 April 2015

The influence of blending $Li_{1.2}Mn_{0.54}Ni_{0.13}Co_{0.13}O_2$ with a small amount of $Na_{0.6}[Li_{0.2}Mn_{0.8}]O_2$ on the electrochemical properties has been investigated. The results indicate that $Na_{0.6}[Li_{0.2}Mn_{0.8}]O_2$ has a beneficial effect on the electrochemical performance of $Li_{1.2}Mn_{0.54}Ni_{0.13}Co_{0.13}O_2$. The initial coulombic efficiency, cyclic performance and rate capability of $Li_{1.2}Mn_{0.54}Ni_{0.13}Co_{0.13}O_2$ have been significantly improved by blending a small amount of $Na_{0.6}[Li_{0.2}Mn_{0.8}]O_2$. Specifically, the $Li_{1.2}Mn_{0.54}Ni_{0.13}Co_{0.13}O_2$ blended with 5 wt% $Na_{0.6}[Li_{0.2}Mn_{0.8}]O_2$ exhibits a discharge capacity of 289 mAh g^{-1} with a coulombic efficiency of 80.1% at the first cycle. The capacity retention is 94.6% at 0.2 C after 50 cycles. Moreover, the discharge capacity increases from 61 to 114 mAh g^{-1} at 5 C. The TEM images show that some $Na_{0.6}[Li_{0.2}Mn_{0.8}]O_2$ particles are partially coated on the surface of the $Li_{1.2}Mn_{0.54}Ni_{0.13}Co_{0.13}O_2$ particles, facilitating to suppress both the oxide ion vacancy elimination and the side reactions with the electrolyte as well as to decrease charge-transfer resistance.

Keywords: Lithium-ion batteries, Cathode material, $Na_{0.6}[Li_{0.2}Mn_{0.8}]O_2$, $Li_{1.2}Mn_{0.54}Ni_{0.13}Co_{0.13}O_2$

1. INTRODUCTION

Several cathode materials, such as $LiCoO_2$, $LiMn_2O_4$, $LiFePO_4$, $LiNi_xCo_yMn_zO_2$, $LiNi_{0.8}Co_{0.15}Al_{0.05}O_2$, have been successfully commercialized since the lithium ion batteries had been put into practical application by using $LiCoO_2$ as cathode material. With the development of hybrid electric vehicles (HEVs) and electric vehicles (EVs), the increasing demand for high-energy and high-

power lithium ion batteries has challenged the commercialized cathode materials. So, developing a cathode material with the high energy density is urgent.

A family of lithium-excess layered manganese-based materials which was regarded as a solid solution between Li_2MnO_3 and $LiMO_2$ (M = Ni, Co, Mn *etc*), has been extensively investigated as a new generation cathode material due to its high energy density as well as inexpensive raw materials [1]. Owning to oxygen extraction from the insulation phase of Li_2MnO_3 during the first charge process, the pristine layered Li-rich cathode materials display a high irreversible capacity loss at the first cycle, a severe capacity fade and poor rate capability during cycling [2–4]. The surface modification [5, 6], acid treatment [7], doping [8] as well as blending with other cathode materials [9] have been proved to alleviate the irreversible capacity loss at the first cycle. Among these approaches, blending with other cathode materials, such as $Li_4Mn_5O_{12}$, LiV_3O_8, V_2O_5, was believed as the effective way to decrease the irreversible capacity loss at the first cycle [10, 11].

Recently, Ke Du *et al*. reported that $Na_{0.6}[Li_{0.2}Mn_{0.8}]O_2$ cathode material delivers an initial discharge capacity of 247 mAh g^{-1} in the voltage range of 2.0–4.8 V though the initial charge capacity is less than 200 mAh g^{-1} [12]. Moreover, the $Na_{0.6}[Li_{0.2}Mn_{0.8}]O_2$ cathode material exhibits an excellent cyclic performance. Attempting to decrease the irreversible capacity loss of the layered lithium-rich cathode materials at the first cycle, we investigated the effect of $Na_{0.6}[Li_{0.2}Mn_{0.8}]O_2$ on the electrochemical performance of $Li_{1.2}Mn_{0.54}Ni_{0.13}Co_{0.13}O_2$ by blending with a small amount of $Na_{0.6}[Li_{0.2}Mn_{0.8}]O_2$. We found that not only initial coulombic efficiency, but also rate capability and cyclic performance of $Li_{1.2}Mn_{0.54}Ni_{0.13}Co_{0.13}O_2$, have been significantly improved by blending $Na_{0.6}[Li_{0.2}Mn_{0.8}]O_2$.

2. EXPERIMENTAL

2.1. Powder preparation and treatment

The layer-structured $Li_{1.2}Mn_{0.54}Ni_{0.13}Co_{0.13}O_2$ was synthesized by a carbonate co-precipitation method followed by high temperature calcination. The spherical precursor of $(Mn_{0.67}Ni_{0.16}Co_{0.16})CO_3$ was prepared as follow steps. Stoichiometric amounts of $MnSO_4 \cdot H_2O$, $NiSO_4 \cdot 6H_2O$ and $CoSO_4 \cdot 7H_2O$ were dissolved in de-ionized water to prepare a 1.0 mol L^{-1} mixed metal ion aqueous. Then the solution was pumped into a continuous stirred tank reactor simultaneously with a Na_2CO_3 solution of 1.0 mol L^{-1} as the precipitator. The concentration of the solution, pH (8.0) and temperature (60 °C) in the reactor were carefully controlled. After reaction, the suspension was aged 2 hours in the water with the temperature of 55 °C. The obtained carbonate precursor was filtered, washed and dried at 120 °C over night. The dry carbonate precursor was thoroughly mixed with stoichiometric Li_2CO_3 (10% excess). The mixed powders were calcined in air for 5 h at 500 °C and then for 12 h at 900 °C to obtain the final product.

The $Na_{0.6}[Li_{0.2}Mn_{0.8}]O_2$ (NLM) compound was synthesized using a traditional solid state method. Stoichiometric amount of Mn_2O_3 (99.0 wt.%), Na_2CO_3 (99.8 wt.%) and Li_2CO_3 (99.9 wt.%)

were thoroughly mixed and then calcinated at 600 °C for 24 h to obtain the desired products. The heating and cooling rates of calcination were 4 and 2 °C min^{-1}, respectively.

The as-prepared $Li_{1.2}Mn_{0.54}Ni_{0.13}Co_{0.13}O_2$ powder (1 g) was mixed with different weight ratios of $Na_{0.6}[Li_{0.2}Mn_{0.8}]O_2$ in the solution of ethanol (50 mL) with help of ultrasonic dispersion for 30 min followed by constantly grinded to be dried. According to the different weight ratios, 3 wt.%, 5 wt.%, 10 wt.% $Na_{0.6}[Li_{0.2}Mn_{0.8}]O_2$ blends were designated as NLM-3, NLM-5, and NLM-10, respectively. The blended powder was heated at 600 °C in air for 5 h with a heating rate of 4 °C min^{-1}.

2.2. Characterization

Powder X-ray diffraction (XRD; Philips, X'pert TROMPD) using Cu Kα radiation (λ= 0.15406nm) at 40 kV/25 mA at 0.06° s^{-1} was employed to characterize the crystal phase of the samples. The surface of the samples was observed by means of transmission electron microscopy (TEM, JEOL 2010). The morphological and composition characterization were performed by scanning electron microscopy (SEM, Hitachi S-4800) and energy dispersive X-ray spectroscopy (EDS).

2.3. Electrochemical measurements

Electrochemical measurements were carried out using CR2023 coin cells. The positive electrodes were prepared by coating slurry containing 80 wt% active materials, 15 wt% carbon black, 5 wt% CMC binder on a Al current collector foils. The typical loading density of prepared electrodes is about 4 mg cm^{-2}. Lithium foil and Celgard 2400 were respectively used as the anode and separator. The electrolyte was 1 M $LiPF_6$ dissolved in DMC: DEC: EC = 1:1:1 (volume). The coin cells were assembled in a glove box filled with Argon. Charge and discharge performances of the cells were investigated using a Neware BTS-610 Tester between 2.0 V and 4.8 V at 30 °C at different rates (1 C = 300 mAh g^{-1}). Electrochemical impedance spectroscopy (EIS) of the cells was obtained from a Zahner Zennium electrochemical workstation at an open circuit voltage, with frequencies from 100 KHz to 10 mHz and perturbation amplitude of 5 mV. Cyclic voltammograms were measured on a LK9805 electrochemical interface at a scanning rate of 0.1 mV s^{-1}.

3. RESULTS AND DISCUSSION

Fig. 1 shows XRD patterns of the pristine $Li_{1.2}Mn_{0.54}Ni_{0.13}Co_{0.13}O_2$, NLM-3, NLM-5, NLM-10 and the pristine $Na_{0.6}[Li_{0.2}Mn_{0.8}]O_2$ (NLM). The pristine $Li_{1.2}Mn_{0.54}Ni_{0.13}Co_{0.13}O_2$, NLM-3 and NLM-5 show the similar XRD patterns. All the peaks can be indexed based on a hexagonal α-$NaFeO_2$ structure with a space group of $R\bar{3}m$ except those between 20° and 25°. Those peaks are caused by super-lattice ordering of the Li, Ni, Co, and Mn in the 3a site, indicating a layered structure with the monoclinic Li_2MnO_3 character (space group $C2/m$) [13, 14]. However, the XRD pattern of NLM is utterly different from those of $Li_{1.2}Mn_{0.54}Ni_{0.13}Co_{0.13}O_2$, NLM-3 and NLM-5, which is in accord with the

XRD pattern of $Na_{0.6}[Li_{0.2}Mn_{0.8}]O_2$ prepared at 600 °C in the previous literature [12]. And, the XRD pattern of NLM-10 is very close to those of $Li_{1.2}Mn_{0.54}Ni_{0.13}Co_{0.13}O_2$, NLM-3 and NLM-5, with exception of peak around 16° represented as the phase of $Na_{0.6}[Li_{0.2}Mn_{0.8}]O_2$. The lattice parameters of four samples are calculated by fitting $R\bar{3}m$ peaks.

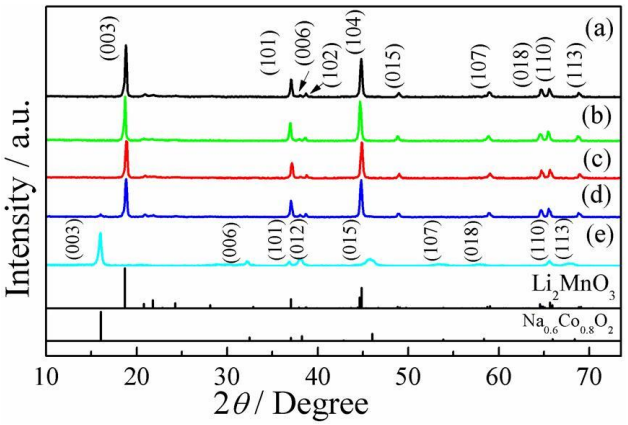

Figure 1. XRD patterns of (a) the pristine $Li_{1.2}Mn_{0.54}Ni_{0.13}Co_{0.13}O_2$ and (b) NLM-3, (c) NLM-5, (d) NLM-10, (e) the pristine $Na_{0.6}[Li_{0.2}Mn_{0.8}]O_2$.

The lattice parameters, ratio values of $I_{(003)}/I_{(104)}$ and the *c/a* ratios are listed in Table 1. In earlier reports [15, 16], the *c/a* ratio was used as the measurement of hexagonality for layered materials. The material possesses layered characteristics when the *c/a* ratio is more than 4.89. In addition, the $I_{(003)}/I_{(104)}$ value was used to determine the cation mixing of a layered material [17, 18]. The *c/a* ratios of four samples are higher than 4.89, indicating four samples possess layered characteristics. However, the ratio of $I_{(003)}/I_{(104)}$ decreases from 1.3514 ($Li_{1.2}Mn_{0.54}Ni_{0.13}Co_{0.13}O_2$) to 1.1287 (NLM-3), 1.1056 (NLM-5) and 1.0363 (NLM-10). Meanwhile, the lattice parameters decrease with the increasing amount of NLM. As reported in recent literature, sodium ions can't substitute any lithium ions in the $Li_{1.2}Mn_{0.54}Ni_{0.13}Co_{0.13}O_2$ because the ion radius of Na^+ (102 pm) is much larger than that of Li^+ (76 pm) [19]. The decrease of $I_{(003)}/I_{(104)}$ ratios and lattice parameters is supposed to be associated with the Li^+ transfer from the pristine $Li_{1.2}Mn_{0.54}Ni_{0.13}Co_{0.13}O_2$ bulk into the NLM bulk due to a calcinations at 600 °C.

Table 1. The unit cell parameters of the pristine $Li_{1.2}Mn_{0.54}Ni_{0.13}Co_{0.13}O_2$, NLM-3, NLM-5, and NLM-10 samples.

Samples	*a* (Å)	*c* (Å)	*c/a*	$I_{(003)}/I_{(104)}$	*V* (Å^3)
The pristine	2.8403	14.1799	4.9925	1.3514	99.07
NLM-3	2.8494	14.2048	4.9852	1.1287	99.88
NLM-5	2.8443	14.1813	4.9860	1.1056	99.35
NLM-10	2.8460	14.1825	4.9833	1.0363	99.48

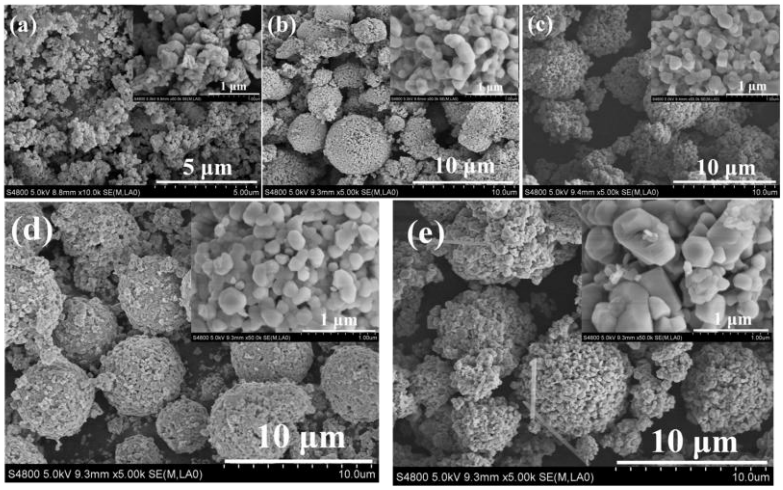

Figure 2. SEM images of (a) $Na_{0.6}[Li_{0.2}Mn_{0.8}]O_2$ and (b) pristine $Li_{1.2}Mn_{0.54}Ni_{0.13}Co_{0.13}O_2$, (c) NLM-3, (d) NLM-5, (e) NLM-10.

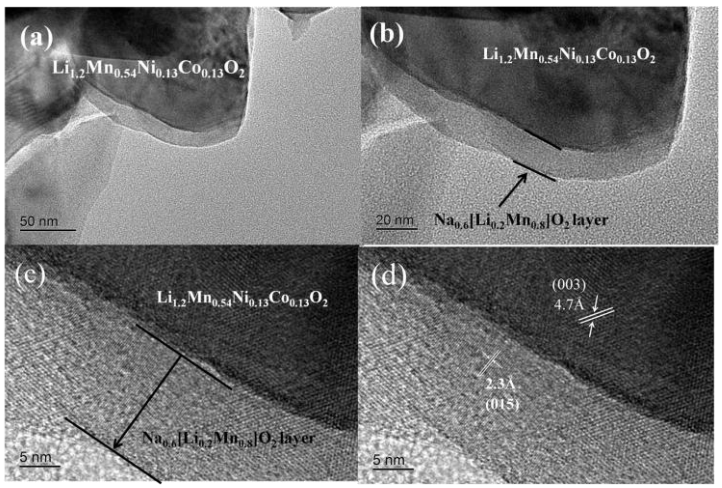

Figure 3. TEM images of NLM-5.

SEM was performed to investigate the morphology of $Na_{0.6}[Li_{0.2}Mn_{0.8}]O_2$, $Li_{1.2}Mn_{0.54}Ni_{0.13}Co_{0.13}O_2$ and $Na_{0.6}[Li_{0.2}Mn_{0.8}]O_2$-blended $Li_{1.2}Mn_{0.54}Ni_{0.13}Co_{0.13}O_2$ samples. As shown in Fig. 2, the morphologies and particle sizes of the $Na_{0.6}[Li_{0.2}Mn_{0.8}]O_2$ powder are utterly different from those of $Li_{1.2}Mn_{0.54}Ni_{0.13}Co_{0.13}O_2$ and $Na_{0.6}[Li_{0.2}Mn_{0.8}]O_2$-blended $Li_{1.2}Mn_{0.54}Ni_{0.13}Co_{0.13}O_2$ samples. The SEM image of $Na_{0.6}[Li_{0.2}Mn_{0.8}]O_2$ shows irregular agglomerations of macro-size primary particles. However, the spherical secondary particles with an average diameter of 4 μm are observed in the SEM images of $Li_{1.2}Mn_{0.54}Ni_{0.13}Co_{0.13}O_2$ and $Na_{0.6}[Li_{0.2}Mn_{0.8}]O_2$-blended $Li_{1.2}Mn_{0.54}Ni_{0.13}Co_{0.13}O_2$ samples. There is no obvious difference in magnification images of the pristine, NLM-3 and NLM-5. Nevertheless, the primary particle size increases when the $Na_{0.6}[Li_{0.2}Mn_{0.8}]O_2$ weight ratio reaches to 10%, which is ascribed to the formation of two phase in one particle when $Na_{0.6}[Li_{0.2}Mn_{0.8}]O_2$-blended $Li_{1.2}Mn_{0.54}Ni_{0.13}Co_{0.13}O_2$ was fired at 600 °C. Fig. 3 is the TEM images of NLM-5. As shown in Fig. 3, the $Li_{1.2}Mn_{0.54}Ni_{0.13}Co_{0.13}O_2$ particle is partially coated by $Na_{0.6}[Li_{0.2}Mn_{0.8}]O_2$.

Table 2. Elemental contents of O, Na, Mn in the pristine $Li_{1.2}Mn_{0.54}Ni_{0.13}Co_{0.13}O_2$ and NLM-5.

Samples	Elemental content (wt.%)		
	O	Na	Mn
The pristine	49.6	0.2	50.2
NLM-5	56.8	2.8	40.4

EDS was conducted to check the distribution of $Na_{0.6}[Li_{0.2}Mn_{0.8}]O_2$ in NLM-5. Fig. 4 shows the energy dispersive X-ray scanning images of the pristine and NLM-5. The Table 2 exhibits the corresponding elemental content of O, Na, Mn. A slight amount of Na is detected in the pristine, which is ascribed to a residual substance of starting material.

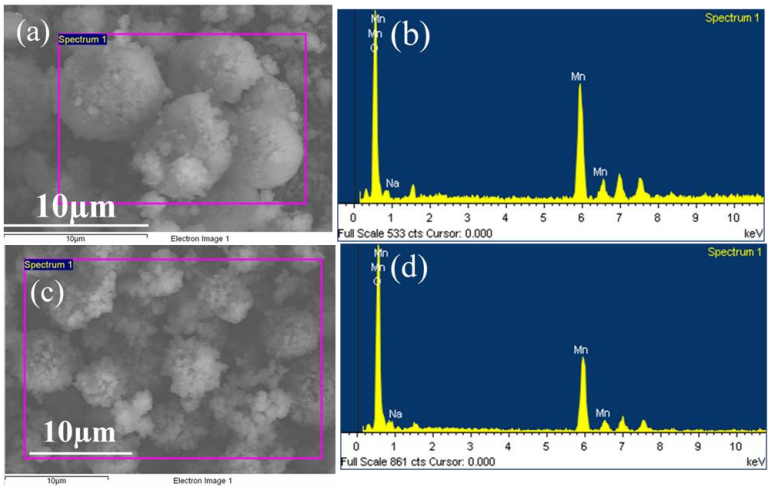

Figure 4. FE-SEM images and Energy dispersive X-ray Scanning images of (a, b) $Li_{1.2}Mn_{0.54}Ni_{0.13}Co_{0.13}O_2$ and (c, d) NLM-5.

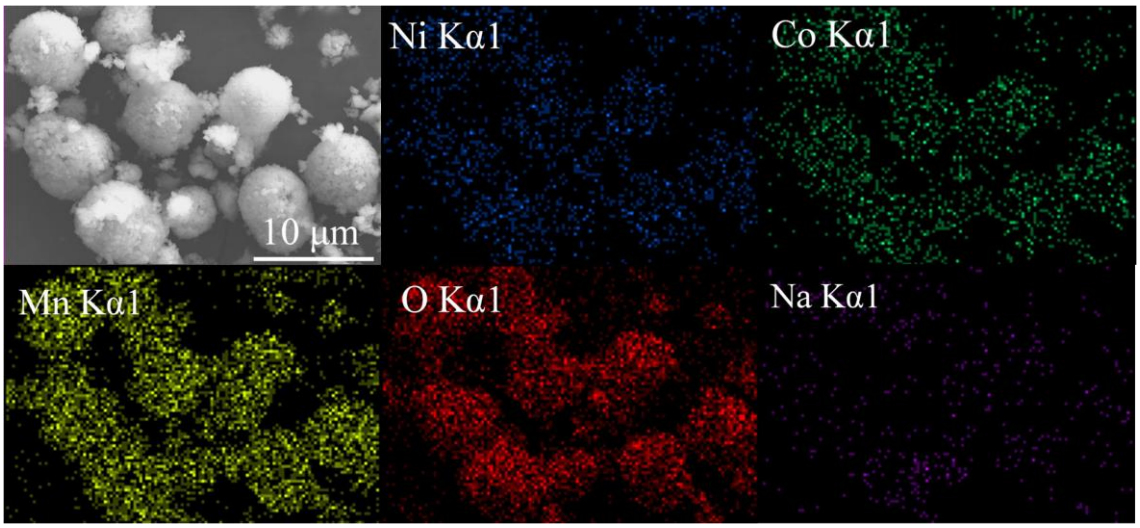

Figure 5. FE-SEM image and EDS dot-mapping for elements of NLM-5.

However, the Na content increases sharply when $Li_{1.2}Mn_{0.54}Ni_{0.13}Co_{0.13}O_2$ was blended with $Na_{0.6}[Li_{0.2}Mn_{0.8}]O_2$. Fig. 5 demonstrates the FE-SEM image and EDS dot-mapping for elements of the NLM-5. As shown in Fig. 5, Na, Ni, Mn, Co and O are homogeneously distributed, indicating a homogeneous distribution of $Na_{0.6}[Li_{0.2}Mn_{0.8}]O_2$ in the $Na_{0.6}[Li_{0.2}Mn_{0.8}]O_2$-blended $Li_{1.2}Mn_{0.54}Ni_{0.13}Co_{0.13}O_2$ sample.

Fig. 6 shows the initial charge/discharge profiles of the electrodes for pristine $Li_{1.2}Mn_{0.54}Ni_{0.13}Co_{0.13}O_2$ and $Na_{0.6}[Li_{0.2}Mn_{0.8}]O_2$-blended $Li_{1.2}Mn_{0.54}Ni_{0.13}Co_{0.13}O_2$ samples at 15 mA g^{-1} (0.05 C) in a voltage range between 2.0 and 4.8 V. Table 3 displays initial charge/discharge capacities and coulombic efficiency. All samples exhibit two plateau regions in the first charge profile, as demonstrated in the other literatures [17, 20, 21]. The slope region is ascribed to the oxidation-reactions of Ni^{2+}/Ni^{4+} as well as Co^{3+}/Co^{4+}. The plateau region above 4.5 V is supposed to be the extraction of Li^+ and removal of O^{2-} from Li_2MnO_3 component[5]. Compared with the pristine $Li_{1.2}Mn_{0.54}Ni_{0.13}Co_{0.13}O_2$, all $Na_{0.6}[Li_{0.2}Mn_{0.8}]O_2$-blended samples deliver a smaller charge capacity and a larger discharge capacity. The pristine exhibits a discharge capacity of 242 mAh g^{-1}. Surprisingly, the discharge capacities of NLM-3, NLM-5 and NLM-10 cathodes are 266, 289 and 255 mAh g^{-1}, respectively. The irreversible capacities of the pristine, NLM-3, NLM-5 and NLM-10 are 156, 74, 72 and 69 mAh g^{-1}, respectively. Both the higher coulombic efficiency and the larger discharge capacity of $Na_{0.6}[Li_{0.2}Mn_{0.8}]O_2$-blended $Li_{1.2}Mn_{0.54}Ni_{0.13}Co_{0.13}O_2$ samples are mainly associated with the $Li_{1.2}Mn_{0.54}Ni_{0.13}Co_{0.13}O_2$ particle is partially coated by $Na_{0.6}[Li_{0.2}Mn_{0.8}]O_2$. As shown in other literature, the coating layer plays a great part on the improvement of the discharge capacity because of suppression of both the oxide ion vacancy elimination and the side reactions with the electrolyte [5, 6, 22]. We infer that the partially coating of $Na_{0.6}[Li_{0.2}Mn_{0.8}]O_2$ on the surface of $Li_{1.2}Mn_{0.54}Ni_{0.13}Co_{0.13}O_2$ can suppress both the oxide ion vacancy elimination and the side reactions with the electrolyte, which contributes to the higher coulombic efficiency and the larger discharge capacity of $Na_{0.6}[Li_{0.2}Mn_{0.8}]O_2$-blended $Li_{1.2}Mn_{0.54}Ni_{0.13}Co_{0.13}O_2$ samples.

Table 3. Initial charge/discharge capacities and corresponding coulombic efficiency of the cathodes for the pristine $Li_{1.2}Mn_{0.54}Ni_{0.13}Co_{0.13}O_2$ and NLM-3, NLM-5, NLM-10 at 15 mA g^{-1} in a voltage range between 2.0 and 4.8 V.

Samples	Charge capacity (mAh g^{-1})	Discharge capacity (mAh g^{-1})	Irreversible capacity (mAh g^{-1})	Coulombic efficiency (%)
The pristine	398	242	156	60.8
NLM-3	340	266	74	78.2
NLM-5	361	289	72	80.1
NLM-10	324	255	69	78.7

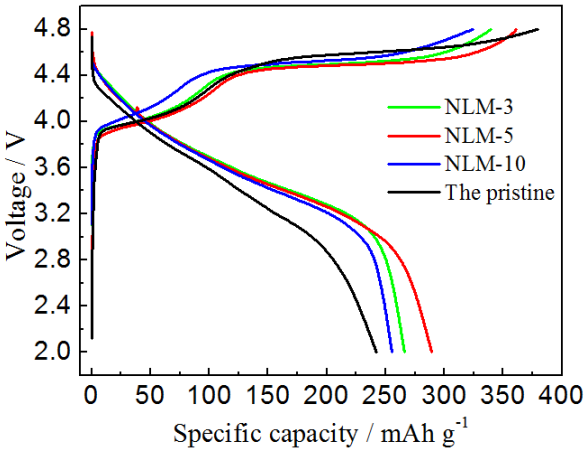

Figure 6. The initial charge/discharge curves of the pristine $Li_{1.2}Mn_{0.54}Ni_{0.13}Co_{0.13}O_2$ and NLM-3, NLM-5, NLM-10.

In order to further understanding the effect of $Na_{0.6}[Li_{0.2}Mn_{0.8}]O_2$ blending in the electrochemical performance of the layered oxide, cyclic voltammetry (CV) test were carried out in this work. The cyclic voltammograms profiles of the pristine and $Na_{0.6}[Li_{0.2}Mn_{0.8}]O_2$-blended $Li_{1.2}Mn_{0.54}Ni_{0.13}Co_{0.13}O_2$ samples were recorded in the voltage range of 2.0–4.9 V at a scan rate of 0.1 mVs^{-1} for the three cycles and are illustrated in Fig. 7a-d. Fig. 7e shows the cyclic voltammograms profiles of the first cycle for the four samples.

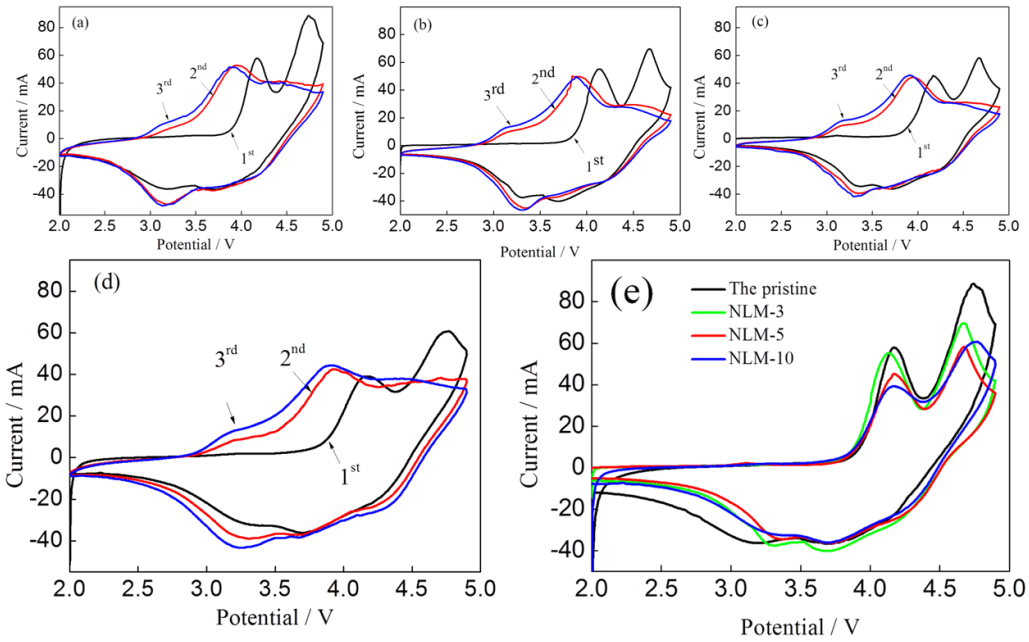

Figure 7. Cyclic voltammograms profiles of (a) the pristine $Li_{1.2}Mn_{0.54}Ni_{0.13}Co_{0.13}O_2$ and (b) NLM-3, (c) NLM-5, (d) NLM-10 and (e) the first cycle of the all samples.

As shown in Fig. 7e, the first anodic peaks of all samples at about 4.0 V are due to the oxidation process of Ni^{2+}/Co^{3+} to higher states. The second anodic peaks located in the potential range between 4.5 V and 4.9 V are attributed to the irreversible electrochemical activation reaction with the extraction of Li_2O from the Li_2MnO_3 component [5, 20, 23, 24]. However, three cathodic peaks are observed in the potential range between 3.0 V and 4.5 V. Two peaks during anodic reactions along with three cathodic peaks are regarded as a complex electrochemical delithiation/lithiation process, which is still not clear at present [6, 25, 24]. What is interesting is that the intensity of the second peak above 4.5 V in the first cycle decreases when $Li_{1.2}Mn_{0.54}Ni_{0.13}Co_{0.13}O_2$ was blended with $Na_{0.6}[Li_{0.2}Mn_{0.8}]O_2$, indicating that the side reaction with electrolyte is suppressed. This result agrees well with the smaller initial charge capacities of NLM-3, NLM-5 and NLM-10.

Figure 8 shows the cyclic performance of the pristine and various wt.% $Na_{0.6}[Li_{0.2}Mn_{0.8}]O_2$-blended $Li_{1.2}Mn_{0.54}Ni_{0.13}Co_{0.13}O_2$ samples at a specific current density of 60 mA g^{-1}. The cells were cycling for 3 times at 15 mA g^{-1} and for 5 times at 30 mA g^{-1}. And then, the cells were cycling for 50 times. The discharge capacity of the pristine $Li_{1.2}Mn_{0.54}Ni_{0.13}Co_{0.13}O_2$ fades from 219 to 186 mAh g^{-1} after 50 cycles and the capacity retention is 85.2%. $Na_{0.6}[Li_{0.2}Mn_{0.8}]O_2$-blended $Li_{1.2}Mn_{0.54}Ni_{0.13}Co_{0.13}O_2$ samples present a better cyclic performance. The capacity retentions of NLM-3, NLM-5 and NLM-10 are 92.1%, 94.6% and 93.5%, respectively. We deduce the enhanced cycling performance of $Na_{0.6}[Li_{0.2}Mn_{0.8}]O_2$-blended $Li_{1.2}Mn_{0.54}Ni_{0.13}Co_{0.13}O_2$ samples can be attributed to the suppression of side reaction with electrolyte which is responsible for the change of charge transfer resistance during cycling.

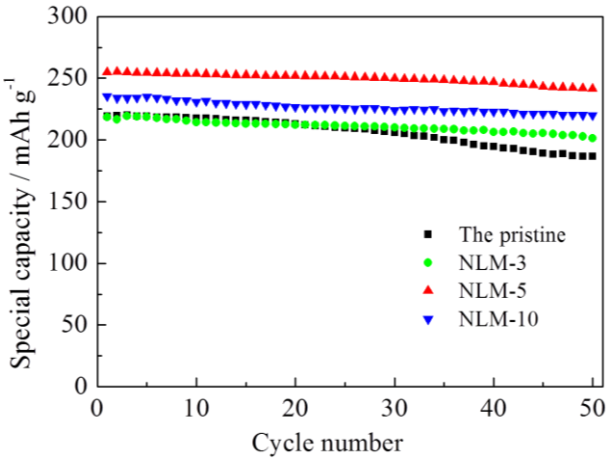

Figure 8. Cyclic performance of the pristine $Li_{1.2}Mn_{0.54}Ni_{0.13}Co_{0.13}O_2$ and NLM-3, NLM-5, NLM-10 at a specific current density of 60 mA g^{-1}.

To examine rate capability of the pristine and various wt.% $Na_{0.6}[Li_{0.2}Mn_{0.8}]O_2$-blended $Li_{1.2}Mn_{0.54}Ni_{0.13}Co_{0.13}O_2$ samples, the cells were cycled at rates of 0.05 C, 0.1 C, 0.2 C, 0.5 C, 1 C, 2 C, 5 C, respectively (1 C = 300 mAh g^{-1}). Fig. 9 shows the rate capability. It is obvious that the $Na_{0.6}[Li_{0.2}Mn_{0.8}]O_2$-blended $Li_{1.2}Mn_{0.54}Ni_{0.13}Co_{0.13}O_2$ samples exhibit a superior rate capability than the pristine $Li_{1.2}Mn_{0.54}Ni_{0.13}Co_{0.13}O_2$. The discharge capacity of the pristine $Li_{1.2}Mn_{0.54}Ni_{0.13}Co_{0.13}O_2$ is 61

mAh g^{-1} at 5 C. At the same current density of 5 C, the discharge capacity of NLM-3, NLM-5 and NLM-10 are 93, 114 and 108 mAh g^{-1}, respectively. The improvement of rate capability is supposed to be related to the enhancement of kinetics caused by the $Na_{0.6}[Li_{0.2}Mn_{0.8}]O_2$ blending. It is reported that the interfaces between $Li_{1.2}Mn_{0.54}Ni_{0.13}Co_{0.13}O_2$ and $Na_{0.7}MnO_{2.05}$ provide the fast diffusion paths for Li^+ [19]. So, it is expected that the interfaces between $Li_{1.2}Mn_{0.54}Ni_{0.13}Co_{0.13}O_2$ and $Na_{0.6}[Li_{0.2}Mn_{0.8}]O_2$ play the same role, which is confirmed by the following EIS measurement.

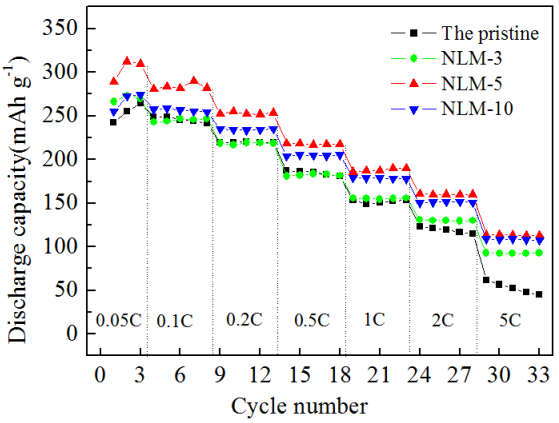

Figure 9. Rate capability of the pristine $Li_{1.2}Mn_{0.54}Ni_{0.13}Co_{0.13}O_2$ and NLM-3, NLM-5, NLM-10.

In order to further understand the kinetic behavior of all as-prepared electrodes, EIS measurements were carried out using the half cells consisting of the pristine $Li_{1.2}Mn_{0.54}Ni_{0.13}Co_{0.13}O_2$ and different wt.% $Na_{0.6}[Li_{0.2}Mn_{0.8}]O_2$-blended $Li_{1.2}Mn_{0.54}Ni_{0.13}Co_{0.13}O_2$ samples as working electrode at the charge state of 4.8 V after the first cycle at 0.05 C and the 50th cycles at 0.2 C. Fig.10 shows the Nyquist plots which consists of a semicircles in high frequency region and a curve in medium frequency region. These plots were fitted by the ZSimpWin software using an equivalent circuit as shown in Fig.11. The semicircle at high frequencies could be attributed to the Li^+ migration resistance (R_f) at the solid electrolyte interphase (SEI) film, a passive layer formed due to the oxidation of electrolyte. The curve at medium frequencies could be attributed to the charge-transfer resistance (R_{ct}) [26]. An intercept at the *Z*real axis in high frequency region corresponds to the ohmic electrolyte resistance (R_e). Constant phase element is employed in the "real world" system in place of a pure capacitor element to reflect the inhomogeneity in the system [27]. A constant phase element CPE_{dl} reflects double layer capacitance and CPE_f presents the capacitance of SEI film. The fitted impedance parameters are listed in Table 4. It is obviously observed that the ohmic electrolyte resistances are similar among the all electrodes. However, the R_f and R_{ct} values of NLM-3, NLM-5 and NLM-10 samples are distinctly smaller than with those of the pristine $Li_{1.2}Mn_{0.54}Ni_{0.13}Co_{0.13}O_2$. This result is accord with that NLM-3, NLM-5 and NLM-10 samples exhibit higher cyclic capacities and better electrochemical properties. Moreover, in contrast to those of the pristine $Li_{1.2}Mn_{0.54}Ni_{0.13}Co_{0.13}O_2$, the R_f and R_{ct} values of NLM-3, NLM-5 and NLM-10 samples increase slowly from the first cycle to the 50th cycle, which is in agreement with our speculation that $Na_{0.6}[Li_{0.2}Mn_{0.8}]O_2$ partially coated on the

surface of the $Li_{1.2}Mn_{0.54}Ni_{0.13}Co_{0.13}O_2$ particle is helpful to suppress interaction between the cathode surface and the electrolyte.

Table 4. The **i**mpedance parameters of the pristine $Li_{1.2}Mn_{0.54}Ni_{0.13}Co_{0.13}O_2$ and NLM-3, NLM-5, NLM-10 cells.

Samples	R_e (Ω cm^2)		R_f (Ω cm^2)		R_{ct} (Ω cm^2)	
	1st	50th	1st	50th	1st	50th
The pristine	5.37	2.31	324.2	473.3	1078	1437
NLM-3	2.59	2.73	157.4	119.3	219.7	257.3
NLM-5	4.51	2.22	42.9	123.4	78.9	131
NLM-10	1.70	1.99	144.8	86.26	175.2	326.3

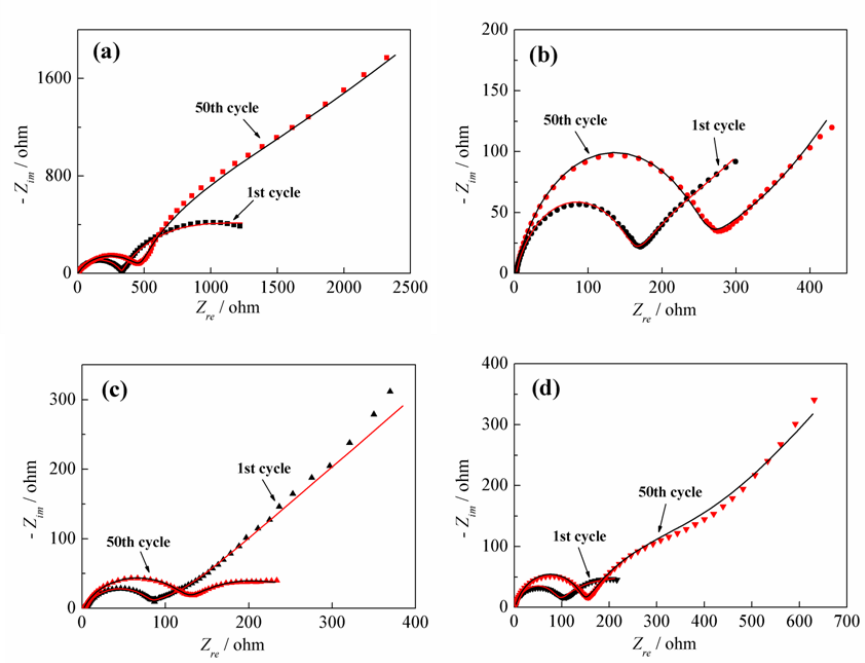

Figure 10. Nyquist plots of (a) the pristine $Li_{1.2}Mn_{0.54}Ni_{0.13}Co_{0.13}O_2$, (b) NLM-3, (c) NLM-5 and (d) NLM-10 cells cycled at the charge state of 4.8 V after initial cycle at 0.05 C and 50 cycles at 0.2C, the real lines in (a) - (d) are the fitting results of the Nyquist plots with the equivalent circuit.

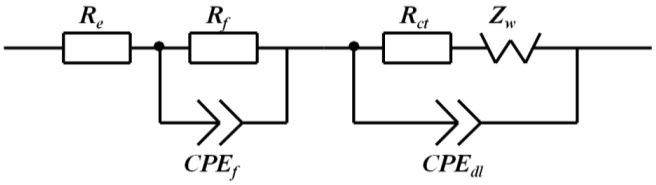

Figure 11. Equivalent circuit of Nyquist plots.

4. CONCLUSION

A small amount blending of $Na_{0.6}[Li_{0.2}Mn_{0.8}]O_2$ is proved to be greatly helpful to the electrochemical performance of $Li_{1.2}Mn_{0.54}Ni_{0.13}Co_{0.13}O_2$. The initial coulombic efficiency, cyclic performance and rate capability of $Li_{1.2}Mn_{0.54}Ni_{0.13}Co_{0.13}O_2$ have been significantly improved by blending $Na_{0.6}[Li_{0.2}Mn_{0.8}]O_2$. The improved initial coulombic efficiency and the larger discharge capacity are attributed to the suppression of the oxide ion vacancy elimination and the side reactions with the electrolyte. The better cyclic performance and rate capability is ascribed to the smaller and relatively stable charge-transfer resistance, which are mainly associated with the partially coating of the $Na_{0.6}[Li_{0.2}Mn_{0.8}]O_2$ on the surface of $Li_{1.2}Mn_{0.54}Ni_{0.13}Co_{0.13}O_2$.

References

1. M.M. Thackeray, C. S. Johnson, J. T. Vaughey, N. Li, & S. A. J. Hackney, *Mater. Chem.* 15 (2005) 2257.
2. S.H. Kang, Y.K. Sun, K. Amine, *Electrochem. Solid-State Lett*. 6 (2003) A183.
3. A.R. Armstrong, M. Holzapfel, P. Novak, C.S. Johnson, S.H. Kang, M.M. Thackeray, P. G. Bruce, *J. Am. Chem. Soc*. 128 (2006) 8694.
4. S. Y. Yang, G. Huang, S. J. Hu, X. H. Hou, Y. Y. Huang, M. Yue, G. T. Lei, *Mater. Lett*. 118 (2014) 8.
5. C. R. Wu, X. P. Fang, X.W. Guo, Y. Mao, J. Ma, C. C. Zhao, *J. Power Sources* 231 (2013) 44.
6. Z. Y. Wang, E. Z. Liu, C. N. He, C. S. Shi, J. J. Li, N. Q. Zhao, *J. Power Sources* 236 (2013) 25.
7. S. H. Kang, C. S. Johnson, J. T. Vaughey, K. Amine, & M.M. Thackeray, *J. Electrochem. Soc*. 153 (2006) A1186.
8. Z. H. Tang, Z. X. Wang, X. H. Li, W. J. Peng, *J. Power Sources* 204 (2012) 187.
9. H. Y. Tran, C. Täubert, M. Fleischhammer, P. Axmann, L. Küppers, M. W. Mehrens, *J. Electrochem. Soc.* 158(5) (2011) A556.
10. J. Gao, A. Manthiram, *J. Power Sources* 191 (2009) 644.
11. J. Gao, J. Kim, A. Manthiram, *Electrochem. Commun*. 11 (2009) 84.
12. K. Du, K. S. Ryu, D. H. Huang, G. R. Hu, *J. Power Sources* 238 (2013) 372.
13. X. Y. Liu, J. L. Liu, T. Huang, A. S. Yu, *Electrochim. Acta* 109 (2013) 52.
14. Z. H. Lu, L. Y. Beaulieu, R. A. Donaberger, C. L. Thomas, J. R. Dahn, *J. Electrochem. Soc*. 149 (2002) A778.
15. Y. Gao, M. V. Yakovleva, W. B. Ebner, *Electrochem. Solid-State Lett*. 1 (3) (1998) 117.
16. J. N. Reimers, E. Rossen, C. D. Jones, J. R. Dahn, *Solid State Ionics* 16 (1993) 335.
17. J. M. Zheng, X. B. Wu, Y. Yang, *Electrochim. Acta* 56 (2011) 3071.
18. K. Karthikeyan, S. Amaresh, G. W. Lee, V. Aravindan, H. Kim, K. S. Kang, W. S. Kim, Y. S. Lee, *Electrochim Acta* 68 (2012) 246.
19. K. Du, F. Yang, G. R. Hu, Z. D. Peng, Y. B. Cao, K. S. Ryu, *J. Power Sources* 244 (2013) 29.
20. S.J.Shi, J.P. Tu, Y.Y. Tang, X. Y. Liu, Y. Q. Zhang, X.L. Wang, C.D. Gu, *Electrochim. Acta* 88 (2013) 671.
21. S.J.Shi, J.P. Tu, Y.Y. Tang, X. Y. Liu, X.Y. Zhao, X.L. Wang, C.D. Gu, *J. Power Sources* 241 (2013) 186.
22. Y. Q. Wu, J. Ming, L. H. Zhou, Y. C. Yu, F. Y. Zhao, *Electrochim. Acta* 113 (2013) 54.
23. L. N. Cong, X. G. Gao, S. C. Ma, X. Guo, Y. P. Zeng, L. H. Tai, R. S. Wang, H. M. Xie, L. Q. Sun, *Electrochim Acta* 115 (2014) 399.
24. Y. H. Wang, X. Yan, X. F. Bie, Q. Fu, F. Du, G. Chen, C. Z. Wang, Y. J. Wei, *Electrochim Acta*

116 (2014) 250.
25. F. Lian, M. Gao, W. H. Qiu, P. Axmann, M. Wohlfahrt-Mehrens, *J Appl Electrochem* 42 (2012) 409.
26. J. Liu, Q. Y. Wang, B. Reeja-Jayan, A. Manthiram, *Electrochem. Commun*. 12 (2010) 750.
27. C. F. Lin, S. F. Song, M. O. Lai, L. Lu, *Electrochim Acta* 143 (2014) 29.